Detection of Extracellular Calcium Gradients with a Calcium-specific Vibrating Electrode

Wiel M. Kühtreiber and Lionel F. Jaffe

Marine Biological Laboratory, Woods Hole, Massachusetts 02543

Abstract. We have developed a vibrating calcium-specific electrode to measure minute extracellular calcium gradients and thus infer the patterns of calcium currents that cross the surface of various cells and tissues. Low-resistance calcium electrodes (routinely ~500 MΩ) are vibrated by means of orthogonally stacked piezoelectrical pushers, driven by a damped square wave at an optimal frequency of 0.5 Hz. Phase-sensitive detection of the electrode signal is performed with either analogue or digital electronics. The resulting data are superimposed on a video image of the preparation that is being measured. Depending on the background calcium concentration, this new device can readily and reliably measure steady extracellular differences of calcium concentration which are as small as 0.01% with spatial and temporal resolutions of a few microns and a few seconds, respectively. The digital version can attain a noise level of less than 1 μV.

In exploratory studies, we have used this device to map and measure the patterns of calcium currents that cross the surface of growing fucoid eggs and tobacco pollen, moving amebae and *Dictyostelium* slugs, recently fertilized ascidian eggs, as well as nurse cells of *Sarcophaga* follicles. This approach should be easily extendable to other specific ion currents.

REPORTS of various biological applications of the vibrating (voltage sensitive) probe (Jaffe and Nuccitelli, 1974) have now appeared in ~200 papers (see Nuccitelli, 1986). This device measures electrical or net charge currents and there is an important class of systems in which it is just these net charge currents that are of the greatest biological significance. These are complex multicellular systems, such as regenerating limb stumps, in which the currents are believed to act by setting up substantial extracellular voltage drops within the tissue (Borgens et al., 1989). However, as Harold (1986) has emphasized, in simpler systems, specific ion currents rather than net charge currents are the parameters of greatest biological significance. With the vibrating voltage sensitive probe, the ions that constitute the currents must be deduced from the effects of various media changes, a rather slow and uncertain procedure. Moreover, the key specific ion currents, such as Ca^{++} currents, may well be only small components of the net charge current, and thus very difficult to study with a conventional vibrating probe. As a first step in improving this method, we have now developed a vibrating calcium-specific electrode.

While ions are often driven across the interior of biological systems by electrical fields, they generally diffuse through the external medium. Such diffusion follows Fick's law:

$$J = -D\,(dc/dx), \qquad (1)$$

where J is an ion flux in the x direction, dc/dx is its concentration gradient, and D is its diffusion constant. Hence it should be possible to map and measure patterns of specific ion flow across a system's surface simply by mapping and measuring this ion's concentration gradients near the surface. Indeed, Kropf et al. (1984) have successfully used this principle, using a nonvibrating pH electrode to determine the pattern of proton currents through growing fungal hyphae. They succeeded without vibration because the background concentration of hydrogen ions was only 0.3 μM which is orders of magnitude lower than that of most other important ions, such as Ca^{++}, in physiological media. Since the sensitivity of any measurement of a concentration difference depends upon the fractional or relative difference (i.e., $\Delta C/C$, not ΔC), their simple method of slowly moving a single probe around a cell would not work at all for most studies. In particular, it would fail for the study of almost all significant steady calcium currents. A survey of the literature shows that estimations of the calcium fluxes in systems as diverse as sea urchin eggs (Azarnia and Chambers, 1976; Jaffe, 1983), fucoid eggs (Robinson and Jaffe, 1975), *Micrasterias* (Troxell et al., 1986), moss buds (Saunders, 1986), and *Drosophila* follicles (Overall and Jaffe, 1985), range from ~1 to >10 pmol/cm² per second (see also Jaffe and Levy, 1987). Considering the calcium background concentrations for the normal extracellular media of such systems (pond water 0.1 mM calcium to seawater 10 mM calcium), the relevant calcium differences to be measured range from 0.01 to 0.2%.

The most serious problem with slowly moving one electrode around a system or putting two separate ones at various pairs of points is voltage drift: one electrode drifts too quickly and two drift independently of each other. One of the

several advantages of a vibrating voltage-sensitive probe is that the probe moves back and forth before significant drift occurs. This also proves to work for vibrating calcium probes. The apparatus described in this paper is based on this principle. A preliminary report on the feasibility of this approach has been published before (Jaffe and Levy, 1987). Since this first effort, the vibrating calcium-selective electrode has been developed into a complete and easy-to-use instrument. In this paper we describe the characteristics of this device, and show preliminary measurements in some biological systems.

Materials and Methods

Construction and Vibration of Calcium Electrodes

Glass micropipettes are pulled from 1.5-mm-diam glass capillaries (TW150-4; World Precision Instruments, Inc., New Haven, CT) on an electrode puller (BB-CH; Mecanex, Geneva, Switzerland) using a two-step pulling procedure. The resulting micropipettes have a stubby appearance with a rather short shank (~2 mm) and a tip diameter of 1–10 μm. The shape of the tip is only slightly conical (see Fig. 1). The micropipettes are silanized with dimethylaminotrimethylsilan vapor (Fluka Chemical Co., Ronkonkoma, NY) for 20 min at 175°C. They are then front filled with 100 mM $CaCl_2$ by applying suction with a syringe. The tip is then front filled with a 4–40-μm-long column of a FLUKA cocktail (Fluka Chemical Co.) containing a calcium-selective sensor, based on the neutral carrier (ETH 1001) of Oehme et al. (1976). Electrical contact is established by inserting a Ag/AgCl wire into the back of the calcium electrode. The return electrode is a Ag/AgCl half cell (World Precision Instruments, Inc.), connected to the solution by a fine tipped pipette filled with 3 M KCl and 0.5% agar. The tip signal is fed into a high impedance voltage follower, which in turn is connected to a ×1,000 amplifier. The DC output of the amplifier is used to determine the response of a stationary electrode to various media.

The performance of our calcium electrodes was evaluated by using them to measure the ionic activity of a dilution series of $CaCl_2$, while their selectivity was assessed with concentrated $MgCl_2$ and KCl solutions (see Table I). The results show that our electrodes have a very linear response with slopes that are close to Nernstian over the whole pCa range that is relevant for extracellular electrodes, and are very calcium selective as evidenced by the results for Mg^{++} and K^+.

The tip resistance of an electrode is estimated by switching a 1 GΩ resistor R_p in parallel with it, and measuring the resulting voltage drop. The resistance R_e of the electrode can then be calculated from

$$R_e = R_p \left(\frac{V_o}{V_i} - 1 \right), \quad (2)$$

Table I. Response of Calcium Electrode

Solution	Electrode potential
	mv
0.01 mM $CaCl_2$	−75.7
0.1 mM $CaCl_2$	−45.3
1 mM $CaCl_2$	−12.8
10 mM $CaCl_2$	19.8
100 mM $CaCl_2$	53.2
100 mM $MgCl_2$	−69.1
100 mM KCl	−100.2

Example of response of a Ca probe (tip resistance ~350 MΩ). Probes were discarded if the slope was below 25 mV. The results for $MgCl_2$ and KCl are consistent with the Ca^{2+} contamination of these chemicals as indicated by the manufacturer.

where V_o is the measured voltage without, and V_i with the parallel resistor switched in.

A calcium-selective electrode is vibrated by an assembly of three piezoelectrical microstages (PZS-100; Burleigh Instruments Inc., Fishers, NY) stacked in orthogonal directions, which is in turn held by a micromanipulator for positioning purposes. The whole setup is built on top of a Zeiss IM35 inverted microscope equipped with a video camera. Because of the very high impedance of the electrode a Faraday cage and an antivibration air table (Micro-G; Technical Manufacturing Corp., Peabody, MA) are necessary to protect it from electrical and mechanical interference. The microstages are driven by a damped square wave at a low frequency (routinely 0.5 Hz). The square wave is produced either by an oscillator (analogue version) or by a computer (see digital version). By controlling the amplitude of vibration of the microstages separately, it is possible to vibrate the electrode at any angle in a two-dimensional plane. We normally vibrate an electrode across rather than along its axis because vibration along the axis somehow introduces artifactual offsets in the measured signals, possibly because of pressure changes on the sensor in the electrode tip.

Measurement of the difference in electrode voltage at the two extremes of vibration is achieved either by using a lock-in amplifier capable of locking in at very low frequencies (analogue version), or by digitizing the electrode signal and computing the potential difference with a computer (digital version). In the latter case, real-time noise reduction is achieved as follows. Since in the digital version the movement of the probe is under computer control, the program knows the position of the probe and therefore a lock-in amplifier is not necessary. After commanding the electrode to move to the other extreme position, the computer takes 1,000 samples (digitizing speed 1 KHz for a vibration frequency of 0.5 Hz), blanks out any transitional

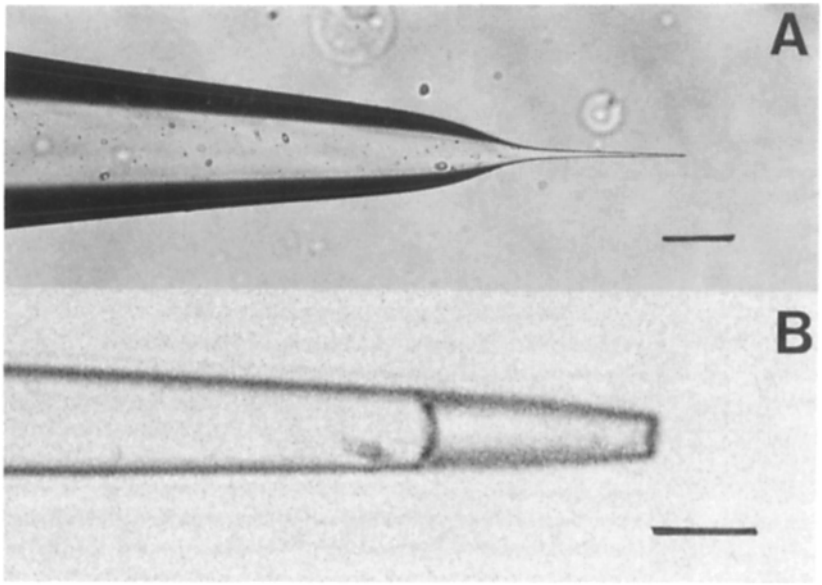

Figure 1. The shape of the tip of the electrodes turns out to be very important for the mechanical stability of the sensor in the tip. If the tip is very conical in shape, the sensor tends to retract from it into the shank. Therefore the best shape is only slightly conical. The best way of pulling such pipettes is a two-step procedure. In the first step the shoulder of the pipette is pulled at a relatively high temperature, whereas the shank and the tip are produced in a second pulling step at a lower temperature. *A* shows the stubby overall appearance of the electrode, whereas *B* shows the tip at higher magnificaton. The sensor is clearly visible. Bars, (*A*) 1 mm; (*B*) 10 μm.

points, and calculates the average. It then calculates the difference between this average and the previous one at the other extreme position and finally calculates a moving average of these differences over any desired time period (comparable to a lock-in time constant). The result is superimposed on the microscope video image ("chart recorder style" or in vector form indicating position, direction of vibration and signal magnitude), and recorded on a timelapse videorecorder as well as on disk. Signal-to-noise ratio, temporal resolution, and overall user-flexibility of the digital system prove to be superior to the (analogue) lock-in based system.

Construction of Artificial Calcium Gradients

To determine the frequency dependence, sensitivity, reproducibility etc. of our vibrating calcium probes, we needed a simple way of generating a range of known, steady calcium gradients without significant voltage gradients. We accomplished this by filling a blunt micropipette (diameter ~10 μm) with 100 mM $CaCl_2$ plus 0.5% agar, placing this in a small petri dish containing the same concentration of $MgCl_2$ plus a certain "background" Ca^{++} concentration (C_B) and waiting about half an hour for a steady state to be set up between Ca^{++} ions diffusing from the reservoir well inside the pipette source and the large sink in the dish. Counter diffusion of Mg^{++} ions minimizes osmotic water flow as well as diffusion potentials, while inclusion of agar avoids bulk flow. Convective disturbances are minimized by placing the tips of the source pipettes as well as the measuring electrode relatively close to the bottom of the dish, actually 100 μm above it.

In the steady state, the extra concentration at the mouth of the pipette, C_o, should be far smaller than the source concentration, C_s deep within it; this because the solid angle inside the pipette's mouth, and thus its diffusional conductance, is so much smaller than the solid angle available for diffusion outside of the pipette's mouth. In actual experiments, C_o is found to be 0.5 to 3% of C_s.

One would expect the steady-state concentration, C at a distance r from such a "point" source in a "semi-infinite" medium to be given by

$$C = C_B + K/r, \tag{3}$$

where C_B is the background concentration and K is an empirical constant that depends on various characteristics of the artificial source. By using a stationary calcium electrode one can easily measure C as a function of r, check Eq. 3, and obtain K (Fig. 2 *top*, Eq. 3A). In the case shown, a nonlinear least square regression yields an equation of the form:

$$C = 0.95 + 9.5/r. \tag{3A}$$

Since the regression has a coefficient of determination of 0.999, the data fit Eq. 3 very well (*solid line* in Fig. 2 *top*).

Differentiation of Eq. 3 then yields the concentration gradient at any distance from the source pipette:

$$\frac{dC}{dr} = \frac{-K}{r^2}. \tag{4}$$

Application of Vibrating Calcium Probes

If a calcium gradient were completely undisturbed by the vibration process and the signal processing system perfect, then

$$\Delta V = S \log \frac{C_2}{C_1}, \tag{5}$$

where S is the Nernstian slope of the electrode, measured as in Table I, and C_1 and C_2 are the calcium concentrations at the two extremes of vibration.

Conversion to natural logarithms gives

$$\Delta V = \frac{S}{2.3} \ln \frac{C_2}{C_1}. \tag{6}$$

Moreover,

$$\ln \frac{C_2}{C_1} = \ln \frac{C_1 + \Delta C}{C_1} = \ln \left(1 + \frac{\Delta C}{C_1}\right). \tag{7}$$

For small values of $\frac{\Delta C}{C_1}$

$$\ln \frac{C_2}{C_1} \cong \frac{\Delta C}{C_{average}}. \tag{8}$$

Substitution in Eq. 6 gives

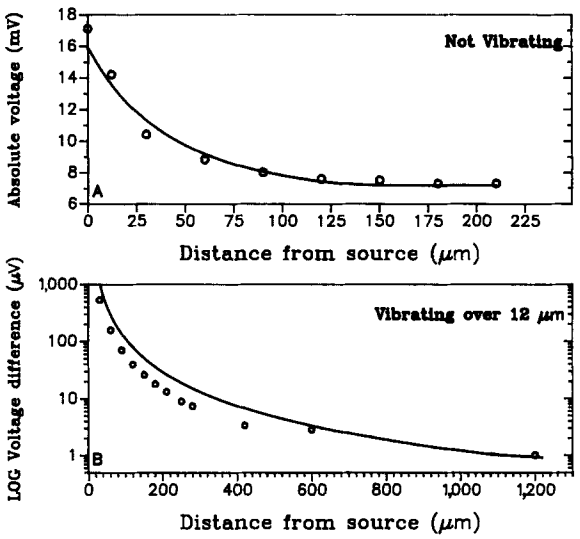

Figure 2. Responses of a vibrating calcium electrode to a calcium gradient set up by the diffusion of calcium out of a source pipette. (*A*) Response of an electrode that is not vibrating. This indicates the change in calcium concentration along the calcium gradient. (*B*) The same gradient as in *A* was explored with a vibrating calcium electrode. The gradient was detectable up to nearly 1 mm away from the source. The open circles represent actual measurements with the probe, whereas the solid line represents the theoretical steady state gradient according to diffusion theory (see text). Artificial source: diameter 10 μm, filled with 100 mM $CaCl_2$ in 0.5% agar. Background calcium concentration = 1 mM $CaCl_2$. Electrode: 40-μm sensor column length; tip diameter, 5 μm. Resistance, 0.8 GΩ. Slope 27.4 mV/decade. Vibration frequency, 0.5 Hz. Vibration amplitude, 12 μm.

$$\Delta V = \frac{S}{2.3} \frac{\Delta C}{C_{average}}. \tag{9}$$

Note that for small signals C_B can be used instead of $C_{average}$. For large signals $C_{average}$ between the two extremes of vibration must be determined.

For electrodes with (nearly) Nernstian slopes, this approximates to:

$$\Delta V \cong 12 \text{ mV } (\Delta C/C). \tag{9A}$$

Substituting Eq. 3 and Eq. 4 in Eq. 9 results in

$$\Delta V = \frac{S}{2.3} \frac{-K \Delta r}{C_B r^2 + Kr}. \tag{10}$$

Using equation (10), a theoretical curve can be drawn, that represents the expected voltage output (*solid line* in Fig. 2 *bottom*).

ΔC can thus be calculated from Eq. 9 or Eq. 9A, using the output of the vibrating calcium probe. Substitution in Fick's law (Eq. 1) then yields the flux (the diffusion constant D for calcium ions in aqueous solutions is 8×10^{-6} cm^2/s [Harned and Owen, 1958]; dx is the vibration amplitude).

Biological Systems and Media

Relevant details pertaining to the measurement of the different biological systems are described in the legends to the figures and tables.

Results

Technical

As already indicated in the introduction, the principle used in the vibrating calcium probe is to eliminate the effects of electrode drift by moving one electrode back and forth be-

tween two positions before drift becomes significant. In an ideal instrument, the signal from such a vibrating calcium probe would be given by Eq. 9; the noise by the thermal or Johnson noise generated by the probe's resistance; the sensitivity by the resulting signal-to-noise ratio.

For a given calcium gradient dc/dx, the signal will depend upon the background concentration C_B and the amplitude of vibration ΔX. The lowest practical value of C_B obviously depends upon the particular biological system and phenomenon being studied. The highest practical value of ΔX depends on whether the signal ΔV increases linearly with ΔX. Data from experiments in which a calcium electrode was vibrated at different amplitudes in an artificial calcium gradient confirm that the response is a linear function of the vibration amplitude (up to at least 30 μm). Note that there is a trade-off between the vibration amplitude ΔX and the spatial resolution. Therefore we usually do not measure at vibration amplitudes exceeding ~30 μm.

Frequency Dependence and System Efficiency

Each time the vibrating probe moves from one position to the other, it drags some fluid at one calcium concentration into fluid at another concentration. Hence one needs to wait long enough, and thus to vibrate slowly enough, to allow diffusion to reestablish the gradient between moves. Moreover, we find that our system generates the largest signal with a somewhat damped square wave (we use a damping half-time of ~30 ms) rather than either a sine wave or a perfect square wave. A sine wave has the obvious disadvantage of spending too little time at the extremes of the vibration where ΔC is greatest; while an undamped square wave may introduce artifacts via turbulence. (The flow patterns with sinusoidal vibration and frequencies of the order of 1 Hz should be laminar since the calculated Reynolds numbers are the order of 10^{-3}.)

By vibrating a calcium electrode at different frequencies within a strong artificial gradient we learned that signal losses do not occur until the frequency exceeds ~0.5 Hz (Fig. 3, see also Table II). At higher frequencies, the signal presumably falls because of incomplete reestablishment of the gradient between moves (see also the legend to Fig. 3).

In Fig. 2 *bottom* we show the result of vibrating a calcium probe, in this optimal way, in the same artificial gradient that was coarsely explored with a fixed probe in Fig. 2 *top*. Over the more reliable part of the curve, between ~100 and 400 μm from the source, the measured signal is consistently about twofold lower than expected. We conclude that our system is less than ideal, so that instead of generating a signal of ~12 mV times the fractional gradient (as predicted by Eq. 9A) it actually generates ~6 mV times this gradient. Thus

$$\Delta C/C \cong \Delta V/6 \text{ mV}.$$

In practice, it is this equation that we use as the basis for calculating calcium fluxes. We believe that the deviation from ideal behavior lies in the measuring system rather than in an error in determining the size of the gradient as described above. We do not know exactly where the measuring system is imperfect, but it seems likely that there is some shortcoming of the electronics at the very low frequencies needed, whereas some failure to completely reestablish the gradient between vibrations, even at 0.5 Hz, may also contribute.

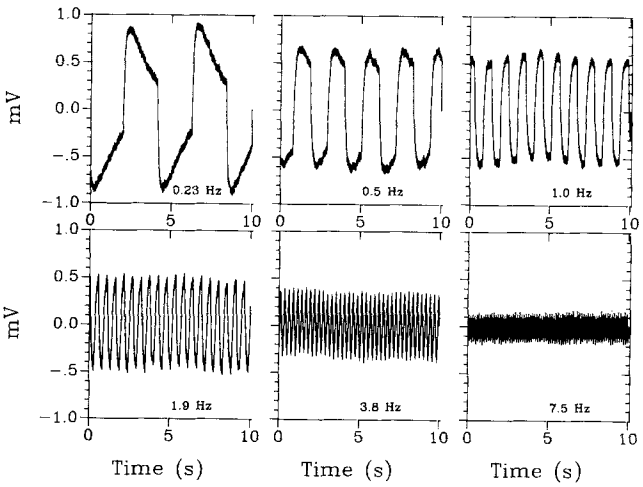

Figure 3. Directly visualized responses of calcium electrodes at different frequencies. Artificial calcium source: 100 mM $CaCl_2$ in 0.5% agar; 10 μm diameter. Background calcium: 0.1 mM $CaCl_2$. Vibration amplitude: 14 μm. The electrode signal was fed into the AC-coupled input of the amplifier. This is to ensure that the electrode drift and the absolute tip potential of the electrode (due to the background calcium concentration) do not cause offsets that are beyond the limits of the amplifier and of the analogue-digital conversion circuitry. AC-coupling has the disadvantage that at low vibration frequencies the tip signal is visibly pulled back toward 0 (especially for 0.23 Hz). However, it can be seen that this effect does not significantly reduce the average voltage difference between the two extremes of vibration. Digitizing was done at a sample speed of 500 Hz, and during 10 s for each frequency.

Probe Resistance, Noise, and Spatial Resolution

Fig. 4 *left* shows the resistances of our calcium electrodes as a function of the lengths of ionophore cocktail column in their tips at different tip diameters. Although the lowest resistances are achieved with very small column lengths, in practice another problem arises: these very small columns appear to last only for a short period of time (<1 h). Also for reasons as yet unknown, these electrodes have higher noise than one would expect from the resistance. One possibility is that very small sensor columns are mechanically somewhat instable. In practice electrodes with a tip diameter of 4 μm and a column length of ~20–30 μm, and thus a resistance of ~0.5 GΩ work very well. Their noise is scarcely distinguishable from that generated by high quality solid state resistors (Fig. 4 *right*). They can be used for 1–2 d and, once stabilized, have a drift of 0.1 mV per hour or less.

The smallest practical tip diameter of our calcium electrodes is ~1 μm. Therefore their attainable spatial resolution (~1 μm) is considerably higher than that of practical voltage-sensitive vibrating probes, which cannot be made smaller than ~5 μm.

Effects of Voltage Gradients

A vibrating calcium probe would surely be expected to register voltage gradients as well as free calcium gradients. However, experience with the voltage-sensitive vibrating probe shows that, over the vibration amplitudes involved, such signals usually are in the nanovolt range; while the vibrating calcium probe only registers signals in the microvolt range

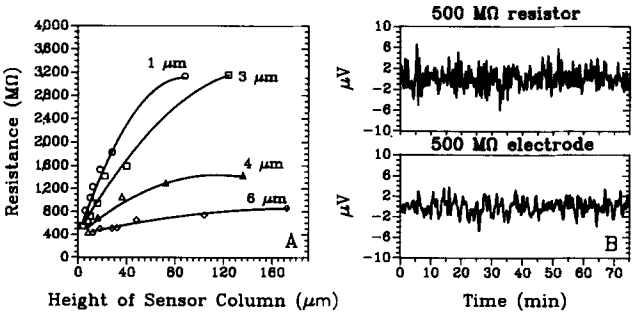

Figure 4. Electrode resistance and noise. (*A*) Resistance versus electrode dimensions. To obtain these data a pipette with a certain tip diameter was repeatedly filled with sensor to various column lengths and the resistance measured. (*B*) The noise after phase-sensitive detection, generated by a 500 MΩ calcium electrode as compared with that of a 500 MΩ solid-state resistor (Victoreen MOX-300; Victoreen Inc., Cleveland, OH).

Table III. Net Performance of Vibrating Calcium Probe

Distance from source	Phase-sensitive detection output uncorrected	Phase-sensitive detection output corrected	Standard deviation	Deviation of mean
μm	*μV*	*μV*	*μV*	*μV*
15	−81.1	−82.8	8.7	2.9
39	−16.2	−17.9	1.6	0.5
73	−2.2	−3.9	0.7	0.2
152	1.4	−0.3	0.6	0.2
285	1.7	0	0.5	0.2

To determine the smallest signal that still can be measured with the vibrating calcium probe, a small artificial calcium gradient was made. In this case, the background concentration calcium was 10 mM. The calcium electrode was vibrated over 10 μm at different distances from the source. Each measurement (which was averaged over 1 min) was repeated 10 times. The 1.7-μV system-offset in the second column is corrected for in the third column. The calcium electrode had a resistance of 320 MΩ.

or higher. Furthermore, in most cases of exceptionally high current densities, where the vibrating voltage-sensitive probe does register signals in the microvolt range, the vibrating calcium probe would be expected to register even higher signals. Nevertheless, exceptional cases can be imagined where voltage gradients may contribute significantly to the observed signal.

A simple test for this possibility would be to raise the vibration frequency of the vibrating calcium probe enough to destroy the calcium gradient. As Table II demonstrates, the component generated by a voltage gradient remains practically unchanged at such increased frequencies. Furthermore, even in most cases where voltage gradients are significant, it should be practical to eliminate them by raising the medium's conductivity with biologically inert ions rather than correcting for the voltage gradient. Suitable ions might include SO_4^{--}, $Tris^+$, and Mg^{++}.

Net Probe Performance

Table III shows the results of repeatedly measuring the calcium gradients generated by a weak artificial source. One can see that with a total measurement time of 10 min gradient-generated voltages as small as 0.5 μV can be detected, while in 1 min ones as small as 5 μV can be easily measured. These correspond to calcium gradients of ~0.01 and 0.1%, respectively.

Table II. Frequency-dependent Response of Vibrating Calcium Probe

Gradient	Vibration frequency					
	Hz					
	0.23	0.5	1.0	1.9	3.8	7.5
Calcium	1	1	0.86	0.64	0.41	0.16
Voltage	1	1	0.98	0.97	0.94	0.82

Comparison of the response of a vibrating calcium electrode to a calcium gradient and its response to a voltage gradient at different frequencies. Values are relative to the slowest frequency used (0.23 Hz). The voltage gradient was 224 μV over 20 μm. The artificial calcium gradient was set up with an artificial source consisting of a micropipette with a tip diameter of 10 μm, containing 100 mM $CaCl_2$ in 0.5% agar. The background calcium concentration for both the calcium gradient and the voltage gradient measurements was 0.1 mM $CaCl_2$.

Biological

We have performed preliminary investigations in a number of biological systems in which calcium fluxes are expected to be found. In the following sections, results are shown to illustrate the usefulness of the vibrating calcium electrode as a new tool to study the functions of calcium. Each system is only illustrated briefly. Full reports will be published separately.

Fucoid Eggs

Eggs of fucoid seaweeds like *Pelvetia fastigiata* drive substantial electrical currents through themselves. Measurements with the vibrating voltage-sensitive probe show that this current first becomes measurable long before outgrowth begins. During growth, the current is found to enter at the growing tip (rhizoid) and to leave at the opposite side (thallus). Ionic substitution studies and $^{45}Ca^{++}$ measurements show that part of this current is due to Ca^{++} ions (maximum 0.03 μA/cm², corresponding to 0.15 pmol/cm² per second; for review, see Jaffe, 1979).

Pelvetia eggs will not initiate tip growth (i.e., germinate) at calcium concentrations much below 1 mM. Hence we have not yet succeeded in measuring calcium currents into the nascent tip. However, after germination, rhizoids grow well down to 10 μM calcium. Thus, as Fig. 5 shows, one can easily measure calcium currents into the growing tip.

This problem illustrates one limitation of the vibrating calcium electrode very clearly: it performs best at low calcium background concentrations, but not all biological material will behave normally under these conditions.

Pollen

Another promising system for investigations with the calcium-specific vibrating electrode is the growing pollen tube. Pollen tubes grow very fast (up to 10 μm per minute), and have been shown to drive a current through themselves with the voltage-sensitive vibrating probe (Weisenseel et al., 1975). Moreover, ^{45}Ca-autoradiography of growing pollen

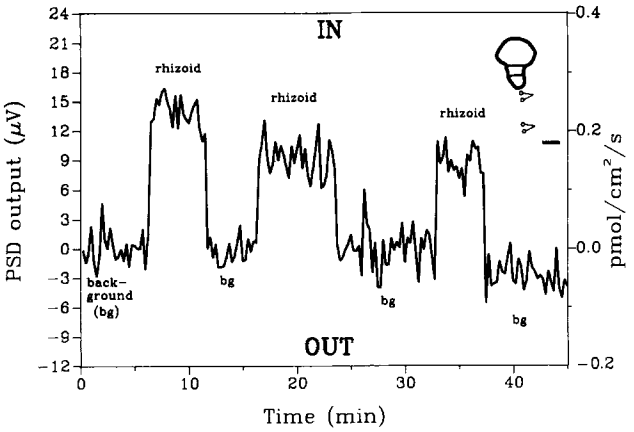

Figure 5. Calcium influx (~0.2 pmol/cm² per second) at the rhizoid tip of a 31-h-old *Pelvetia fastigiata* embryo. The measurements were performed in low calcium artificial seawater containing a final concentration of 10 μM Ca^{++}. Such a small flux can be registered by the calcium probe because of the low concentration of background calcium. No calcium flux was detectable at the thallus side. *bg*, background measurement. The inset shows a screen drawing with the calcium electrode vibrating near the rhizoid and in a background position. Vibration amplitude not drawn to scale. Bar, (*inset*) 50 μm.

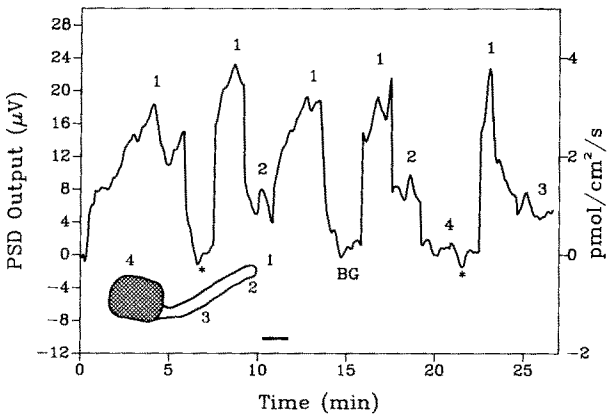

Figure 6. Calcium influx (~4 pmol/cm² per second) at the growing tip of a *Tobacco* pollen tube. Growth speed is normal at the calcium concentration used (0.1 mM). The influx is highest at the tip (*1*) and much reduced at the flanks of the tube (*2* and *3*). The * indicates vibration parallel to the calcium gradient in position *1*. *BG*, background measurement. No calcium flux was detectable at the pollen grain itself (*4*). See inset for the positions. Bar, (*inset*) 10 μm.

tubes shows that calcium accumulates within the growing tip (Jaffe et al., 1975). According to Weisenseel et al. (1975), the maximum (inward) current density at the tip of the growing lily pollen tube is ~500 nA/cm². If this would all be calcium, this would correspond to a flux density of ~2.5 pmol/cm² per second. (1 pmol/cm² per second Ca^{++} corresponds to 193 nA/cm²).

Measurements with the vibrating calcium probe on tobacco pollen show an inward tip current of ~4 pmol/cm² per second that corresponds to ~800 nA/cm² and thus accounts for most or all of the measured electrical current. Moreover, Weisenseel et al. (1975) report an outgoing current with a maximum density of ~350 nA/cm² at the grain itself, where the vibrating calcium probe does not detect any signal. Clearly this outward grain current must be carried by an ion different from calcium. Moreover, this result also confirms that the signals measured with the vibrating calcium probe are really due to calcium and not to voltage gradients (Fig. 6).

Dictyostelium

It is well known from measurements in shaking cultures of the cellular slime mold *Dictyostelium discoideum* that components are released by the cells in a periodic manner during differentiation from the growth phase to the aggregative state, so as to generate sinusoidal oscillations in extracellular pH, cAMP, cGMP, calcium, potassium, and other components (see Bumann et al., 1986). Much less is known about the aggregation stage and moving slug stage, since these are less accessible to the methods used at the amoeboid stage. $^{45}Ca^{++}$ autoradiography of slugs shows that the net calcium concentration of the anterior (prestalk) region is higher than of posterior (prespore) region, while it is also known that high extracellular calcium concentrations induce stalk differentiation (see Maeda and Maeda, 1973).

With the vibrating calcium electrode it is now possible to directly investigate calcium fluxes at these later stages (Fig. 7). The markedly reduced influx in the anterior (prestalk) region is of particular interest (Fig. 7 *C*).

Amebae

Nuccitelli et al. (1977) have shown that a relatively steady current with an average surface density of 0.1–0.2 μA/cm² enters the tail of an ameba and leaves at its pseudopods. This steady current is reduced when the [Ca^{++}] in the medium is reduced. From this it was concluded that Ca^{++} ions carry much of this inward current, although it could not be excluded that the decrease in external calcium somehow decreased the fluxes of other ions such as Cl^- (Nucitelli et al., 1977). Aequorin injections into amebae also show that shape changes of the migrating ameba are accompanied by (ill-defined) rises in the intracellular [Ca^{++}] (Kuroda et al., 1988; Taylor et al., 1980).

With the vibrating calcium probe we have now been able to show directly that there is a (small) calcium influx from the extracellular medium into the ameba (Fig. 8; Table IV). As expected for such a highly dynamic system with frequent directional changes as the amoeba, the rate and location of calcium influx is highly variable, as evidenced by the very high standard deviations in the table. Influx accounts for the majority of the signals measured. Sometimes brief periods of efflux (much larger in magnitude than for influxes) were found, especially in polypodial forms (data not shown). While calcium appears to move into all parts of the ameba, the largest average influx is measured at the tail.

Sarcophaga bullata Follicle

The fleshfly *Sarcophaga bullata* has vitellogenic, polytrophic follicles in which 1 oocyte and 15 nurse cells form a syncytium that is organized in a morphologically as well as physiologically polarized system. Studies with the voltage-sensitive vibrating probe have shown that current is directed

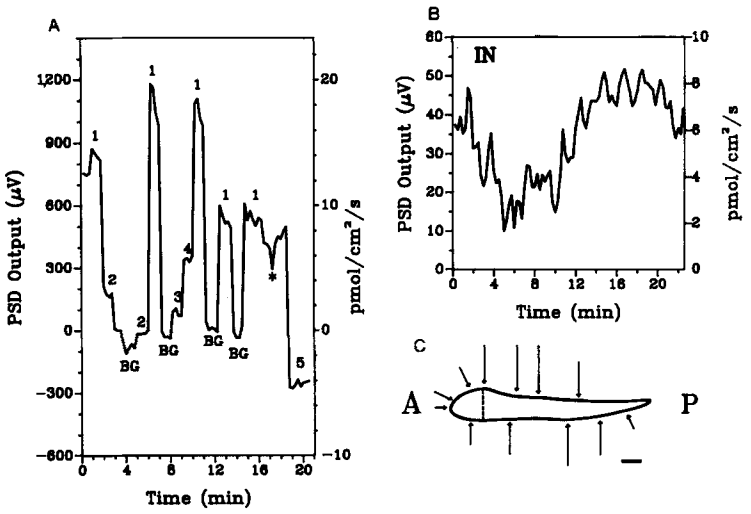

Figure 7. (*A*) Calcium influx into a *Dictyostelium discoideum* slug. Calcium currents were measured in distilled water + 10 μM $CaCl_2$. Differentiation proceeds normally in this medium. *1*, vibration perpendicular to anterior tip. *2*, vibration parallel to anterior tip. The signal is small because the calcium electrode now vibrates perpendicularly to the calcium gradient and therefore the calcium concentration at both extremes of vibration are (approximately) the same. *3*, 100 μm away from anterior tip. *4*, 50 μm away from anterior tip. *5*, perpendicular to posterior tip. *BG*, background measurement. At the *, the slug moved away from the electrode, after which the electrode was repositioned closer to the slug. (*B*) Oscillations of the calcium flux into the tip of a slug. The periodicity is in agreement with values given for calcium oscillations in the literature (Bumann et al., 1986). (*C*) Diagram showing a representative distribution of calcium fluxes in a slug. While there is an overall influx, it is much smaller at the anterior (and also somewhat at the posterior) end of the slug. The dashed line indicates the expected borderline between prestalk and prespore cells for the *Dictyostelium* strain (NC4) used (MacWilliams and Bonner, 1979). *A*, anterior; *P*, posterior side of the slug.

outward over the oocyte surface and directed inward over most of the nurse cell compartment. Ionic substitution studies show that an increase of $[K^+]$ in the extracellular ringer medium decreases the current densities and even causes reversal of the current direction. However, manipulation of the $[Ca^{++}]$ and addition of the calcium antagonist gadolinium have no obvious effect on the electric field (Verachtert, 1988).

Measurements with the calcium probe show that there is a small efflux of calcium from the nurse cells (Fig. 9). This may explain why the manipulation of calcium as described above had no effect: Since the Ca^{++} movement is directed outward, it is expected to be largely independent of the (low) external calcium concentrations.

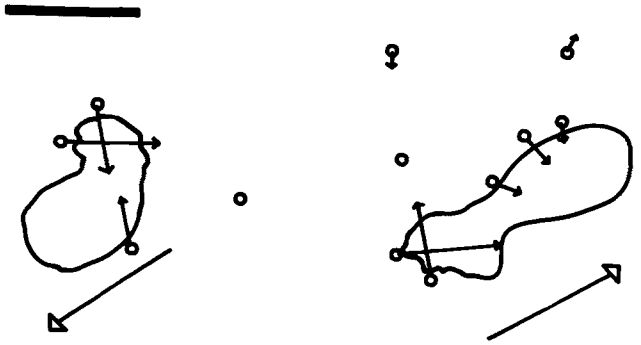

Figure 8. Screen drawings showing representative distributions of calcium fluxes in an *Amoeba proteus*. Since the ameba is moving relatively fast, only a limited number of measurements can be made before the change in shape and/or position becomes too obvious. The angles of the vectors indicate the direction of vibration of the calcium electrode, whereas their length is an indication of the flux. The large arrows indicate the general directions of movement of the amebae. The open circle at one end of each vector indicates the position of the calcium electrode at that time. Each vector represents the mean of 10 s worth of measuring (total measuring time ~1 min for left and ~2 min for right ameba). The tail-ends exhibit the largest fluxes under the conditions used. The flux pattern is polarized tail to front most of the time. The long axis of the left ameba is ~150 μm. Bar, 10 μV.

Phallusia mammilata

In eggs of a variety of species, fertilization results in a large transient increase in the cytoplasmic free calcium concentration, after which the developmental block of the mature egg is released, and development commences. Using the calcium-specific photoprotein aequorin, Speksnijder et al. (1989) have shown that this is also the case for eggs of *Phallusia mammilata*, even in the complete absence of external calcium (i.e., in the presence of 5 mM EGTA plus contamination calcium only). Speksnijder et al. (1989) concluded that most, if not all, of the calcium required for the fertilization pulse is released from internal stores.

Table IV. Calcium Fluxes in Amoeba proteus

	Phase sensitive detection output	Flux
	μV	*fmol/cm²/s*
Front	6.6 ± 4.2	44 ± 28
Front/side	10 ± 1.3	67 ± 9
Side	2.8 ± 1.4	19 ± 9
Tail/side	6.9 ± 0.2	46 ± 1
Tail	16.8 ± 6.9	112 ± 46
Background	0.5 ± 2.7	3 ± 18

Representative fluxes into monopodial *Amoeba proteus* at pH 5.5. The numbers indicate the mean influxes and their standard deviations. The calcium signals in amebae are very small and are only measurable because the background calcium concentration can be made so low (down to 1 μM and lower) without interfering with the movement of the amebae. Signals that were clearly distinguishable from background were obtained at a background concentration of 10 μM Ca^{++}. The voltage probe results indicate a largest current density of 0.2 μA/cm². For a medium with a resistivity of 5,000 Ωcm this corresponds to a voltage difference of 1 μV at a vibration amplitude of 10 μm. This means that the expected voltage component in the calcium flux measurements is ~1 μV. This should vanish in the noise. So the signals at 10 μM are clearly not due to voltage gradients. (10 μM Ca^{++} Marshall's medium: 0.15 mM K_2HPO_4, 0.11 mM KH_2PO_4, 0.01 mM $CaCl_2$, 0.05 mM $MgSO_4$, 0.49 mM $MgCl_2$. Adjust to pH 5.5 with H_2SO_4 [modified from Bruce and Marshall, 1965, to reduce calcium while keeping Cl^- constant].)

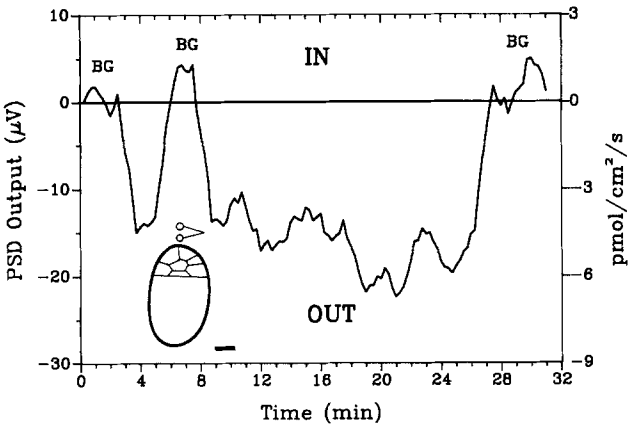

Figure 9. Calcium efflux at the apex of the nurse cell cap of a 4C stage *Sarcophaga bullata* follicle. Measurements were made in normal *Sarcophaga* ringer with 10 times reduced calcium (calcium concentration 0.22 mM; normal ringer composition is 121.5 mM NaCl, 10.0 mM KCl, 1.0 mM NaH_2PO_4, 10.0 mM $NaHCO_3$, 0.7 mM $MgCl_2$, 2.2 mM $CaCl_2$, pH 6.8). The vibration amplitude is not drawn to scale. Bar, (*inset*) 100 μm.

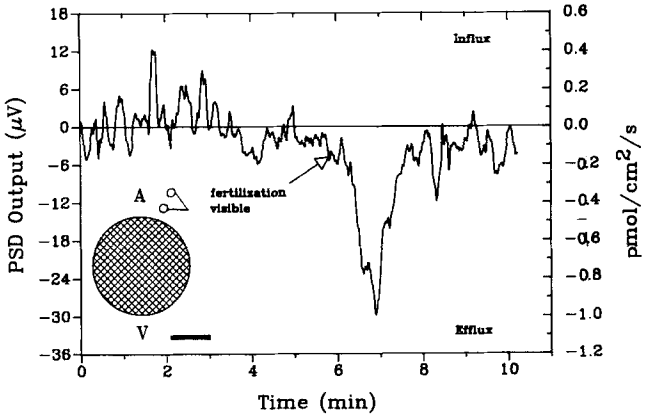

Figure 10. Calcium efflux during fertilization of *Phallusia mammilata*. The dechorionated egg was inseminated with sperm that were "preactivated" according to Sardet et al. (1989) with chorionated eggs in normal (millipore filtered) seawater for 30 min. 30 μl of concentrated sperm activated in this way were added to a dish containing 3 ml calcium-free artificial seawater (CaFSW). Finally, a few eggs, rinsed in CaFSW, were added. This point in time is the insemination time. The final calcium concentration after insemination was measured to be 26 μM. The probe was positioned close to the animal pole of the egg. As soon as the contraction wave of fertilization became visible (*arrow*), a transient efflux of calcium became apparent. *A*, animal pole; *V*, vegetal pole. The vibration amplitude is not drawn to scale. Bar, (*inset*) 50 μm.

Measurements with the calcium specific vibrating electrode show that the egg actually loses calcium during fertilization, as would be expected if internal stores release calcium into the cytosol (Fig. 10). The duration of the calcium efflux is ~2 min, which corresponds to the duration (2–3 min) of the rise in cytosolic free calcium as reported by Speksnijder et al. (1989).

Discussion

Instrumental Considerations

We can now reliably map and measure extracellular calcium ion gradients as small as 0.1% over distances as small as 1 μm and for times as small as a few seconds. To some extent of course there is a trade-off between amplitude resolution, spatial resolution, and temporal resolution: one cannot attain all three of these limits at once. The primary purpose of such measurements is to study patterns of calcium flow through the surfaces of developing cells and organisms; gradients are easily converted into fluxes via Fick's law.

The only earlier application of this principle that we know of has been to the study of proton currents. In a pioneering study, Kropf et al. (1984) have used a nonvibrating pH electrode to determine the pattern of proton currents through growing fungal hyphae. Examination of Fig. 7 in Kropf et al. (1984) indicates that pH differences as small as 0.01 pH unit could be reliably detected. This corresponds to a detection limit or amplitude resolution of ~2%, whereas the detection limit of a vibrating calcium electrode is ~0.5 μV/6 mV or 0.01%. Moreover, the spatial and temporal resolution in the study of Kropf et al. (1984) was ~50 μm and min, respectively. Altogether the amplitude, space, and time resolutions of the vibrating calcium electrodes are the order of 100 times better.

Only very limited further improvements in the resolving power of our system would seem to be attainable. With regard to amplitude resolution, our system now registers about half the attainable signal and seems to be very close to the Johnson noise limit. With regard to spatial resolution, one could certainly fabricate calcium electrodes smaller than 1 μm in diameter; however, the attendant rise in resistance and hence Johnson noise together with the needed reduction in vibration amplitude would reduce the signal-to-noise ratio and hence the amplitude resolution to levels so low as to make smaller electrodes pointless except in very unusual circumstances. With regard to temporal resolution, one is presently limited by the time needed for diffusion to reestablish a gradient after the probe moves. We could imagine reducing this time by embedding cells in a thixotropic gel which would let the probe carry a thinner layer of medium from one point to the other as it moves. However, preliminary efforts to do this were defeated by artifactual signals of unknown origin. Furthermore, for the measurement of rapid ionic events, there is little or no point in vibrating the probe at all since electrode drift is not a problem for measuring fast signals.

Biological Considerations

In interpreting such measurements it is important to realize that the inferred calcium fluxes in any system may have components that cross the plasma membrane via vesicles as well as ones that cross it directly; this because many secretory vesicles are known to contain high net calcium concentrations (Njus et al., 1986; Table I). Thus the main components of the large net influxes of calcium into the tips of growing pollen tubes and fucoid rhizoids seem likely to be a large influx through calcium ion channels minus a substantial efflux carried by the secretory vesicles which generate the growing cell wall. The small efflux of calcium from the *Sarcophaga* nurse cell compartment is also probably due to secretion.

On the other hand, the sharply reduced influx of calcium into the anterior, prestalk cell region of *Dictyostelium* slugs might imaginably result from vesicles that support localized slime secretion; although it might also represent local inhibition of an influx through calcium channels by higher cytosolic calcium levels in prestalk cells. In any case, the different dynamic balance in *Dictyostelium* probably reflects its unusual natural environment. It lives in or on water films which are exceptionally impoverished in calcium. Under these circumstances it seems likely to obtain the high cortical calcium needed for secretion from internal sources (ultimately fed by ingested bacteria) rather than through calcium channels from the environment. This in turn would be expected to favor the evolution of control circuits in which high cortical calcium would act to reduce influx rather than result from greater influx. In short, the reduced calcium influx found in the front part of *Dictyostelium* slugs seems likely to reflect higher rather than lower cytosolic calcium there.

The pulse of net calcium efflux in just fertilized *Phallusia* eggs presumably results from the large release of internal calcium into the cytosol during fertilization (Speksnijder et al., 1989). However, unlike other eggs, the ascidian egg does not respond to fertilization with an obvious burst of exocytosis. So the observed efflux probably occurs via accelerated pumping rather than vesicular transport.

Finally, the faster influx of calcium into the tails of monopodial amebae is also likely to be nonvesicular. For one thing, in the simple salines used, pinocytosis is known to be extremely slow (Cooper, 1968); for another, vesicular uptake would not account for the net charge currents that enter amoeba tails (Nuccitelli et al., 1977).

Future Developments

Perusal of Fluka's Biochemika Handbook indicates that this method should be readily extendable to hydrogen, magnesium, potassium, and sodium ions simply by changing cocktails. Extension to hydrogen or pH gradients and thus to proton currents is particularly attractive because of the very low background concentrations of this ion in most media. Indeed, it is because their medium contained only 0.3 μM hydrogen ions that Kropt et al. (1984) were able to measure pH gradients and infer proton currents through *Achlya* hyphae, even with a nonvibrating electrode.

The authors wish to thank Al Shipley for his technical support. Phillip C. Williams has provided invaluable help in the design of our analog electronics, and Richard Sanger in the digital version. Annelies Speksnijder and Christian Sardet helped with the *Phallusia* experiments. Barend Verachtert helped with the *Sarcophaga* experiments. Peter Hepler provided the tobacco pollen.

Financial support was provided by National Institutes of Health, National Science Foundation, and United States Department of Agriculture grants to L. F. Jaffe.

Received for publication 4 December 1989 and in revised form 22 January 1990.

References

Azarnia, R., and E. L. Chambers. 1976. The role of divalent cations in activation of the sea urchin egg. I. Effect of fertilization on divalent cation content. *J. Exp. Zool.* 198:65–77.

Borgens, R. B., K. R. Robinson, J. W. Vanable, and M. E. McGrinnis. 1989. Electrical Fields In Vertebrate Repair. Alan R. Liss, Inc., New York. 310 pp.

Bruce, D. L., and J. M. Marshall. 1965. Some ionic and bioelectric properties of the amoeba *Chaos*. *J. Gen. Physiol.* 49:151–178.

Bumann, J., D. Malchow, and B. Wurster. 1986. Oscillations of Ca^{++} concentration during the cell differentiation of *Dictyostelium discoideum*. *Differentiation.* 31:85–91.

Cooper, B. A. 1968. Quantitative studies of pinocytosis induced in *Amoeba proteus* by simple cations. *C. R. Trav. Lab. Carlsberg.* 36:385–403.

Harned, H. S., and B. B. Owen. 1958. The Physical Chemistry of Electrolyte Solutions. Reinhold, New York. 259.

Harold, F. M. 1986. Transcellular ion currents in tip-growing organisms: where are they taking us? *In* Ionic Currents in Development. R. Nuccitelli, editor. Alan R. Liss, Inc., New York. 359–366.

Jaffe, L. A., M. H. Weisenseel, and L. F. Jaffe. 1975. Calcium accumulations within the growing tips of pollen tubes. *J. Cell Biol.* 67:488–492.

Jaffe, L. F. 1979. Control of development by ionic currents. *In* Membrane Transduction Mechanisms. R. A. Cone and J. E. Dowling, editors. Raven Press, Ltd., New York.

Jaffe, L. F. 1983. Sources of calcium in egg activation: a review and hypothesis. *Dev. Biol.* 99:265–276.

Jaffe, L. F., and S. Levy. 1987. Calcium gradients measured with a vibrating calcium-selective electrode. *IEEE (Inst. Elect. Elect. Eng. Med. Biol. Soc.) Conf.* 9:779–781.

Jaffe, L. F., and R. Nuccitelli. 1974. An ultrasensitive vibrating probe for measuring steady extracellular currents. *J. Cell Biol.* 63:614–628.

Kropf, D. L., J. H. Caldwell, N. A. R. Gow, and F. M. Harold. 1984. Transcellular ion currents in the watermold *Achlya*. Amino acid proton symport as a mechanism of current entry. *J. Cell Biol.* 99:486–496.

Kuroda, K., Y. Yoshimoto, and Y. Hiramoto. 1988. Temporal and spatial localization of Ca^{2+} in moving *Amoeba proteus* visualized with aequorin. *Protoplasma.* 144:64–67.

MacWilliams, H. K., and J. T. Bonner. 1979. The prestalk-prespore pattern in cellular slime molds. *Differentiation.* 14:1–22.

Maeda, Y., and M. Maeda. 1973. The calcium content of the cellular slime mold, *Dictyostelium discoideum*, during development and differentiation. *Exp. Cell Res.* 82:125–130.

Njus, D., P. M. Kelley, and G. J. Harnadek. 1986. Bioenergetics of secretory vesicles. *Biochim. Biophys. Acta.* 853:237–265.

Nuccitelli, R. 1986. Ionic Currents in Development. Alan R. Liss, Inc., New York. 375 pp.

Nuccitelli, R., M.-M. Poo, and L. F. Jaffe. 1977. Relations between ameboid movement and membrane-controlled electrical currents. *J. Gen. Physiol.* 69:73–76.

Oehme, M., M. Kessler, and W. Simon. 1976. Neutral carrier Ca^{++} microelectrodes. *Chimia.* 30:204–206.

Overall, R., and L. F. Jaffe. 1985. Patterns of ionic current through *Drosophila* follicles and eggs. *Dev. Biol.* 108:102–119.

Robinson, R., and L. F. Jaffe. 1975. Polarizing fucoid eggs drive a calcium current through themselves. *Science (Wash. DC).* 187:70–72.

Sardet, C., J. E. Speksnijder, I. Inoué, and L. F. Jaffe. 1989. Fertilization and ooplasmic movements in the ascidian egg. *Development.* 105:237–249.

Saunders, M. J. 1986. Cytokinin activation and redistribution of plasmamembrane ion channels in *Funaria*. *Planta (Berl.).* 167:402–409.

Speksnijder, J. E., D. W. Corson, C. Sardet, and L. F. Jaffe. 1989. Free calcium pulses following fertilization in the ascidian egg. *Dev. Biol.* 135: 182–190.

Taylor, D. L., J. R. Blinks, and G. Reynolds. 1980. Contractile basis of amoeboid movement. VIII. Aequorin luminescence during amoeboid movement, endocytosis, and capping. *J. Cell Biol.* 86:599–607.

Troxell, C. L., C. Scheffey, and J. D. Pickett-Heaps. 1986. Ionic currents during wall morphogenesis in *Micrasterias* and *Closterium*. *In* Ion Currents in Development. R. Nuccitelli, editor. Alan R. Liss, Inc., New York. 105–112.

Verachtert, B. 1988. Electrical polarity in the ovarian follicles of *Sarcophaga bullata*, *Drosophila melanogaster* and *Locusta migratoria*. Ph.D. thesis, University of Leuven, Leuven, Belgium. 207 pp.

Weisenseel, M. H., R. Nuccitelli, and L. F. Jaffe. 1975. Large electrical currents traverse growing pollen tubes. *J. Cell Biol.* 66:556–567.